Journal of Energy and Power Engineering 5 (2011) 1053-1062

Simulation of Solar Radiation Conditions in Coastal and Continental Areas by Using a New Algorithm

P. Monowe and N. Nijegorodov

Department of Physics, University of Botswana, Private Bag 0022, Gaborone, Botswana

Received: February 17, 2011 / Accepted: June 09, 2011 / Published: November 30, 2011.

Abstract: An algorithm developed at the University of Botswana is used to study solar radiation conditions in Namibia, South Africa, Mozambique and Botswana. The synoptic stations chosen for the study differ by meteorological conditions and location: some are in coastal areas and others are in continental locations. The simulation results reveal that daily direct beam solar radiation, H_{bn}, is usually higher in the continental area than in the coastal one. The same situation is observed with daily global solar radiation, H_g. The difference becomes even larger for partly cloudy weather, because in coastal areas sunshine hours are usually less than in continental areas. Furthermore, coastal areas have higher humidity and bigger air mass compared to continental locations. It is concluded that continental areas are more convenient for utilisation of solar energy using solar devices with concentrators (middle-temperature and high-temperature Rankine cycles), while at coastal areas flat-plate collectors and PV-arrays are preferable. It is found out that the range of optimum slopes for SADC countries studied is from +30° to -62°.

Key words: Simulation, solar radiation, optimum slope, SADC countries, coastal, continental.

1. Introduction

Southern Africa Development Community (SADC) consists of fifteen member states. The current study focuses on four selected countries, namely Botswana, Mozambique, Namibia and South Africa.

Botswana is land-locked at the centre of Southern Africa. It lies roughly between latitudes 18°-27°S and longitudes 20°-29°E. The climate is mainly semi-arid to arid. Summer days (October to March) are hot with temperatures in the 38-41 ℃ range. Winter days (April to September) are clear-sky, dry and cool to warm; however evening and night temperatures can drop below freezing point especially in the south west.

Mozambique is located on the eastern coast of Southern Africa between latitudes 10°12' and 26°52' and longitudes 30°12' and 40°51'E. On the eastern coast, the Indian Ocean stretches over 2470 km. The climate is predominantly tropical. The hot season is from September to April and the cool season is from May to August. The climate of Mozambique is to a large extent influenced by: coastal conditions, the easterly winds and the mountain. In June-July the winds blow from the Indian Ocean. In December-January two streams of winds meet at the Intertropical Convergence Zone (ITCZ).

Namibia lies in the western coast of Southern Africa, bordering the south Atlantic Ocean. The geographical coordinates are roughly 22°S and 17°E, with the northern border at approximately 17°S and the southern boarder at approximately 28°S. The coastline is 1572 km. The climate is desert, with hot dry days with sparse and erratic rainfall.

South Africa occupies the southern tip of Africa. Its average coordinates are latitudes 29°00'S and longitude 24°00'E. It has long coastline of more than 2500 km that stretches from the desert border with Namibia along the Atlantic Ocean, southwards around the tip of Africa, and then northwards to the border with Mozambique along the Indian Ocean. The climate of South Africa is

Corresponding author: P. Monowe, lecturer, research fields: power energy systems, modelling and simulations, materials science. E-mail: monowep@mopipi.ub.bw.

classified as semi-arid but varies with topology.

All the countries discussed above have abundant solar energy. However, the availability of solar radiation in SADC countries has not been sufficiently studied, especially in coastal areas, though there are some published works concerning continental areas. For example, Gopinathan [1] used the well known Page [2] relations and some other relations given in Refs. [3, 4] to investigate the distribution of global and sky radiation at 12 locations in Lesotho. Lewis [5] did the estimation of irradiance for 6 locations in Zambia, while Hove and Göttsche [6] have done a systematic experimental investigation of solar radiation components in Zimbabwe. Madhlopa [7] investigated the monthly average daily and seasonal daily clearness indices for one weather station in Malawi. In the few instances where studies were conducted covering more than one country in the SADC region, for example in Refs. [8, 9], the work was confined to continental areas. To the authors' knowledge, there are no reported comprehensive investigations of solar radiation conditions in coastal areas of SADC countries. In this paper a comparison of simulated solar radiation components at both continental and coastal areas is made and analysed.

2. The Algorithm Used

The algorithm used simulates the instantaneous, hourly, daily and monthly mean direct normal, diffuse and global components of solar radiation and to predict daily mean and monthly mean optimum slopes is based on previous work by Nijegorodov et al. [10-14]. The algorithm allows simulating of all solar radiation parameters if a slope, β, is known. If β is unknown the programme simulates the optimum slope β_{opt}, which is obtained by maximising the daily total insolation on an inclined surface with respect to the slope, that is,

$$\left[\frac{d}{d\beta}(H_T)\right]/\beta_{opt} = 0 \qquad (1)$$

A schematic representation of the algorithm is given in Fig. 1. The solar constant, I_s is considered to be 1367 $W \cdot m^{-2}$ [15]. Input data are: temperature T, relative humidity RH, sunshine hours S, visibility V, and thickness of the ozone layer D_o. The solar radiation parameter can be daily mean, if the solar components are simulated for a particular day, or monthly mean daily if monthly mean daily components are simulated for the Julian. Standard values can be used (V = 23 km and D_o = 0.34 cm) [16, 17], for cases where visibility and thickness of the ozone layer are unknown. Location and date input data are: latitude ϕ, altitude A, date D and month M. The third set of input data are: surface azimuth angle γ, slope β and ground albedo ρ. Detailed description of the algorithm used in this paper is given in Ref. [18]. The algorithm and software used are based on the laws of spectroscopy, kinetic theory and thermodynamics. This algorithm facilitates the study of monthly mean solar radiation components and monthly

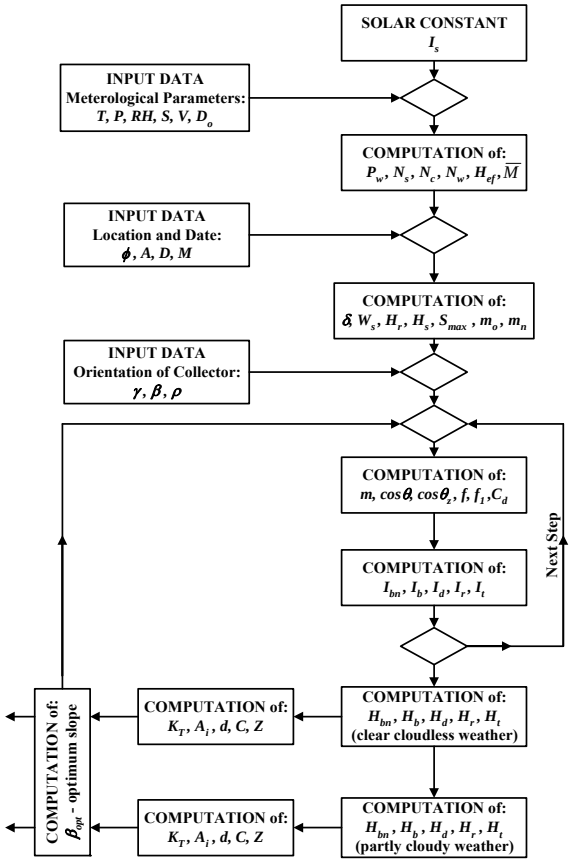

Fig. 1 Schematic representation of the algorithm to simulate hourly, daily and monthly mean daily solar radiation components and optimum slopes (notations are defined in Ref. [18]).

optimum slopes, and it was applied for some locations in Namibia, Botswana, South Africa and Mozambique.

3. Results and Discussion

3.1 Experimental Investigation of the Validity of the New Algorithm and Software Used

To check the validity of the algorithm and software used only completely clear and cloudless days, from sunrise to sunset moments, were chosen. Such days were observed to be 12th and 25th November. Experimental values of hourly direct beam, I_{bn}, global, I_g, and diffuse, I_d, solar radiation components were recorded using EPLAB equipment namely: normal incidence pyrheliometer (model NIP) with solar tracker (model ST-3), two precision spectral pyranometers (models PSP) one of them with shading ring. Simulations were done for meteorological conditions measured at solar noon, because for the Gaborone location, during November the difference between solar noon and local time noon is negligible.

A comparison of the experimental I_{bn}, I_g, and I_d components recorded on 12th November, with the simulated results is shown in Fig. 2, wherein experimental graphs are represented by solid lines and simulated ones by dashed lines. Meteorological conditions on 12th November were: (a) Temperature was increasing during daytime, from 25 ℃ at 6:00 to 36 ℃ at 18:00. At solar noon it was 34 ℃; (b) Relative humidity was decreasing from 40% at 6:00 to 32% at 18:00. At solar noon it was equal to 34%. (c) Visibility was a standard one (V = 23 km) until 15:30 and then it was slowly decreasing due to dust stirred by wind from the Kalahari Desert. The sky dome was cloudless but a little bit milky. It is evident from Fig. 2, that overall, there is a very good match between experimental and simulated results; though in the afternoon, starting from 16:00, experimental values of I_{bn} are slightly lower than simulated ones. This difference could be attributed to the decreasing visibility from 16:00. The discrepancies between experimental and simulated results for hourly solar radiation components on 12th November at 12:00 are: 0.2% for I_{bn}, 0.9 % for I_g and

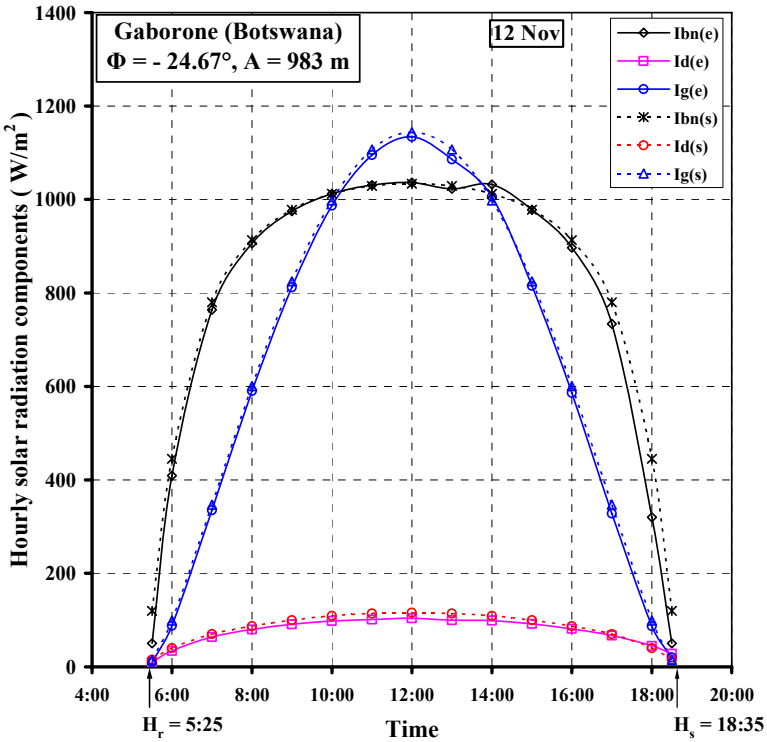

Fig. 2 Comparison of experimental and simulated hourly solar radiation components for Gaborone (ϕ = -24.67°, A = 983 m) on 12 November. I_{bn}, I_d and I_g are the hourly direct beam, diffuse and global radiation, respectively. Subscripts (e) and (s) denote experimental and simulated, respectively.

11.5% for I_d. For the daily components, the discrepancies are: 2.1% for H_{bn}, 1.7% for H_g and 9.5% for H_d.

The comparison of the experimental I_{bn}, I_g, and I_d components with simulated ones for 25th November is shown in Fig. 3. On this day, the sky dome was cloudless and extremely clear, dark blue in colour. Meteorological conditions on 25th November were: (a) Temperature was increasing during daytime, from 24 ℃ at 6:00 to 31 ℃ at 18:00. At solar noon it was 29 ℃; (b) Relative humidity was decreasing from 43% at 6:00 to 34% at 18:00. At solar noon it was 39%. (c) Visibility in the morning was 65-70 km and during daytime it increased to 75-80 km. It is observed from Fig. 3 that there is a very good agreement between the experimental and simulated results. The discrepancies between hourly solar radiation components on 25th November at 12:00 are: 0.1% for I_{bn}, 0.6% for I_g and 4.3% for I_d. For the daily components, the discrepancies are: 0.14% for H_{bn}, 0.3% for H_g and 3.9% for H_d.

On the basis of foregoing comparisons between the experimental and simulated results, the algorithm and software used for subsequent simulation of solar radiation components and other related parameters is deemed to be valid and reliable with acceptable discrepancy ranges.

3.2 Simulations of Solar Radiation Components and Daily Optimum Slopes

The results of the simulations show that there is a big difference between solar radiation components for continental and coastal locations in some SADC countries.

Some examples of the variation of the daily solar radiation components (H_{bn}, H_b, H_g and H_d) are presented in Fig. 4. It is noted that for a typical continental location like Tsabong (Botswana), with average sunshine hours of 9.67 h/day, the daily direct beam component, H_{bn}, vary between 45.34 MJ·m^{-2}·day^{-1}

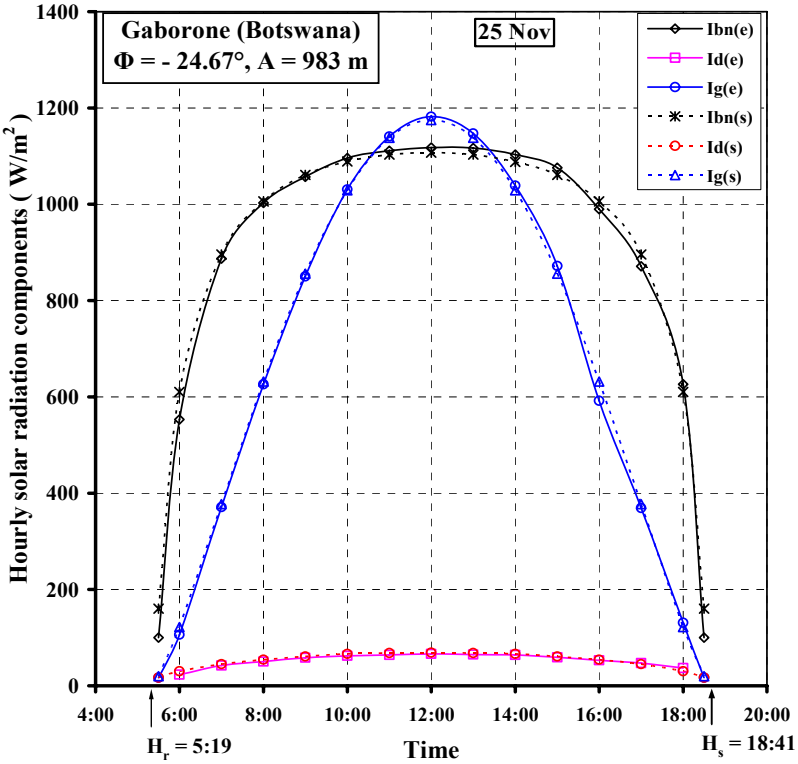

Fig. 3 Comparison of experimental and simulated hourly solar radiation components for Gaborone (ϕ = -24.67°, A = 983 m) on 25 November. I_{bn}, I_d and I_g are the hourly direct beam, diffuse and global radiation, respectively. Subscripts (e) and (s) denote experimental and simulated, respectively.

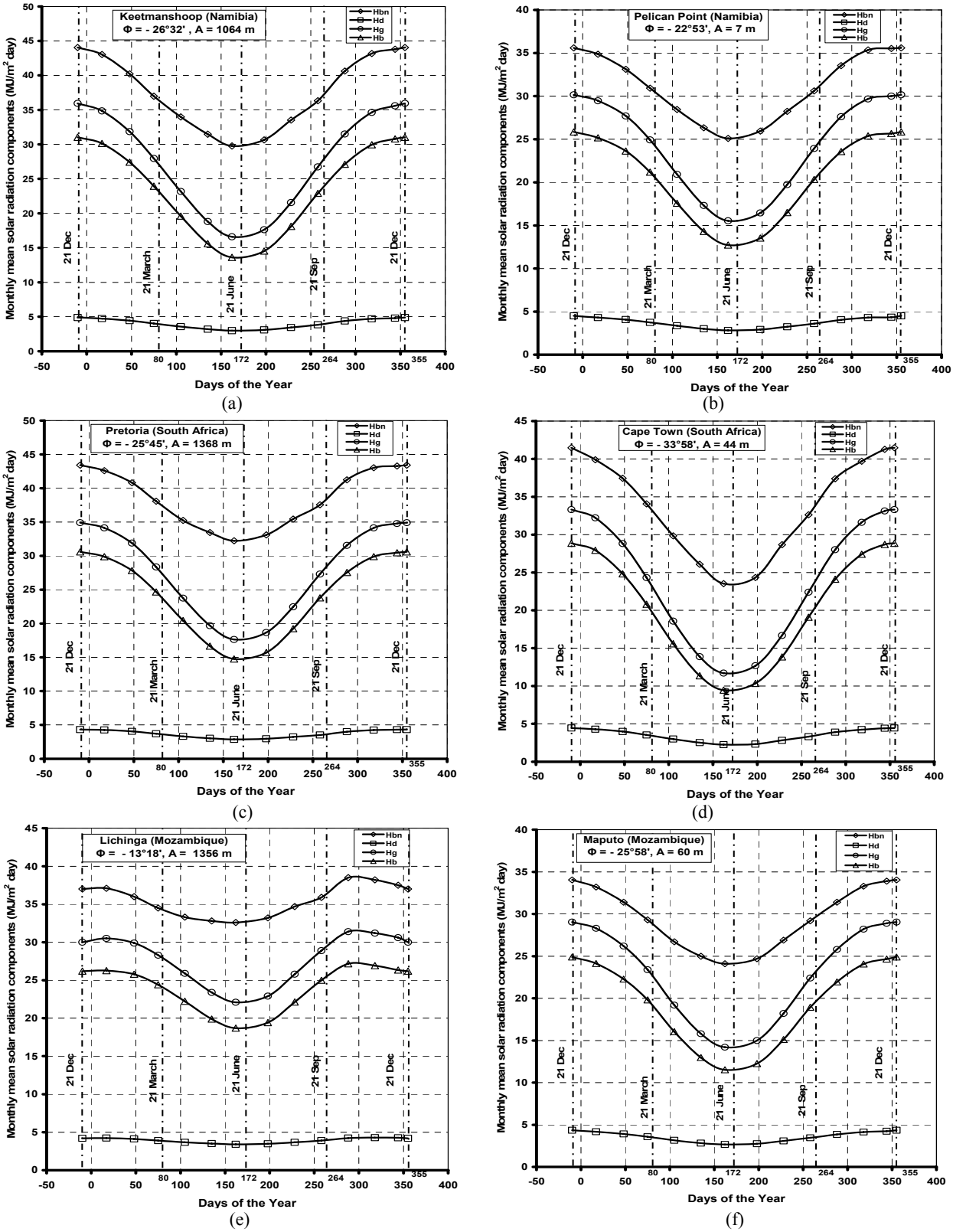

Fig. 4 Variation of mean daily solar radiation components for: (a) Keetmanshoop, (b) Pelican Point, (c) Pretoria, (d) Cape Town, (e) Lichinga, and (f) Maputo. H_{bn}, H_d, H_g and H_b are the daily direct beam, diffuse, global and beam on horizontal radiation, respectively. The points represent mean monthly daily solar radiation. (Monthly mean meteorological parameters were used in the simulations).

(at 21 December) and 32.25 MJ·m^{-2}·day^{-1} (at 21 June) and the daily global component, H_g, vary between 36.23 MJ·m^{-2}·day^{-1} (at 21 December) and 17.57 MJ·m^{-2}·day^{-1} (at 21 June). The mean annual values, $\overline{H}_{bn}$ and $\overline{H}_g$ are equal to 38.83 MJ·m^{-2}·day^{-1} and 27.52 MJ·m^{-2}·day^{-1}, respectively. For partly cloudy weather (for mean monthly meteorological conditions) these parameters are 31.27 MJ·m^{-2}·day^{-1} and 23.21 MJ m^{-2}·day^{-1}. Such high values of $\overline{H}_{bn}$ and $\overline{H}_g$ provide excellent opportunities for utilisation of solar energy using devices with concentrators as well as plain collectors and PV-arrays.

If we consider Keetmanshoop location (Namibia) which is also far from the coast, we found a similar trend of results for H_{bn} and H_g. For this location H_{bn} varies between 44.04 MJ·m^{-2}·day^{-1} (at 21 December) and 29.80 MJ·m^{-2}·day^{-1} (at 21 June). Similarly, H_g varies from 39.54 MJ·m^{-2}·day^{-1} (at 21 December) to 13.65 MJ·m^{-2}·day^{-1} (at 21 June). However, if Pelican Point (Namibia), a coastal location, is considered, then H_{bn} and H_g components are found to be much lower. At Pelican Point H_{bn} varies between 35.55 MJ·m^{-2}·day^{-1} (21 December) and 25.10 MJ·m^{-2}·day^{-1} (21 June), and H_g varies between 30.15 MJ·m^{-2}·day^{-1} (at 21 December) and 12.70 MJ·m^{-2}·day^{-1} (at 21 June).

Furthermore, if we compare locations in South Africa, for example, either Cape Town location with Kimberly or Durban location with Pretoria we observe the same pattern of results: at continental locations (Pretoria and Kimberly) H_{bn} and H_g components are higher than at coastal areas (Cape Town and Durban). For instance, at Pretoria H_{bn} varies between 43.41 MJ·m^{-2}·day^{-1} (at 21 December) and 32.24 MJ·m^{-2}·day^{-1} (at 21 June), while H_g varies from 34.91 MJ·m^{-2}·day^{-1} to 17.63 MJ·m^{-2}·day^{-1}. On the other hand, at Cape Town H_{bn} varies from 41.48 MJ·m^{-2}·day^{-1} (at 21 December) to 23.41 MJ·m^{-2}·day^{-1} (at 21 June), whereas H_g varies between 33.31 MJ·m^{-2}·day^{-1} and 11.75 MJ·m^{-2}·day^{-1}.

Three factors are identified as being responsible for these results. Firstly, humidity is usually high at coastal areas. It affects solar radiation components due to two specific processes: absorption of solar radiation by water molecules and by scattering of solar radiation by the air turbidity. Thus the increase in humidity leads to an increase in the number of water molecules in the atmosphere column, hence more solar radiation would be absorbed. This causes a decrease in direct beam radiation, H_{bn}. At the same time the increase in humidity increases the turbidity of the air, and hence there is an increase in the scattering of solar radiation. This results in a decrease in direct beam radiation, while diffuse radiation, H_d, increases. Secondly, the air mass, which decreases with altitude, is the biggest at sea level. The air mass of the atmosphere increases all kinds of attenuation of solar radiation by the atmosphere. Thirdly, it is observed that solar radiation components at coastal areas also affected by prevailing winds which carry clouds and hence, decrease sunshine hours.

A typical example of the effect of prevailing winds (Fig. 5) upon solar radiation pattern is observed in Mozambique. The simulated results for the 21 synoptic stations have been analysed and are presented in Fig. 6, in the form of maps of monthly mean daily direct beam radiation for December and June. The background to the information presented about Mozambique, in Figs. 5 and 6, has been discussed in detail in Ref. [18]. However, the effect of prevailing trade winds upon solar radiation patterns could be common in coastal areas of other SADC countries, particularly Tanzania, South Africa, Namibia and Angola.

The variations of daily optimum slopes with days of the year for six synoptic stations mentioned at Fig. 4 are shown in Fig. 7. The solid curves in this figure represent the variation of the daily optimum slopes with days of the year, the dots on the curve represent mean monthly optimum slopes, and the shaded areas represent the manifold of optimum slopes for different clear cloudless hours. For example, if the sky is completely covered by clouds, then the optimum slope becomes zero (in order to intercept all diffuse radiation). The sign "+" means that the collector should

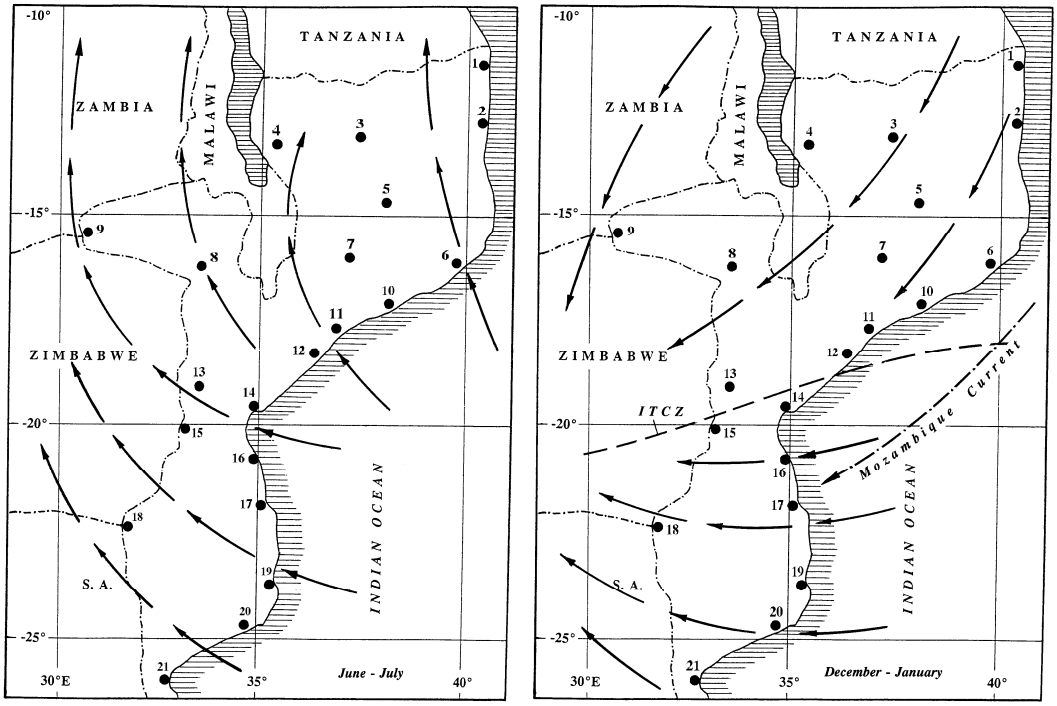

(a) (b)

Fig. 5 Easterly winds over Mozambique in (a) June-July and (b) December-January. The numbered dots are the synoptic stations: (1) Mocimboa da Praia, (2) Pemba, (3) Marrupa, (4) Lichinga, (5) Ribane, (6) Angoche, (7) Errego, (8) Tete, (9) Zumbo, (10) Pebane, (11) Quelime, (12) Chinde, (13) Chimoio, (14) Beira, (15) Espungabera, (16) Nova Mambone, (17) Vilanculos, (18) Chicualacuala, (19) Inhambane, (20) Quissico, and (21) Maputo.

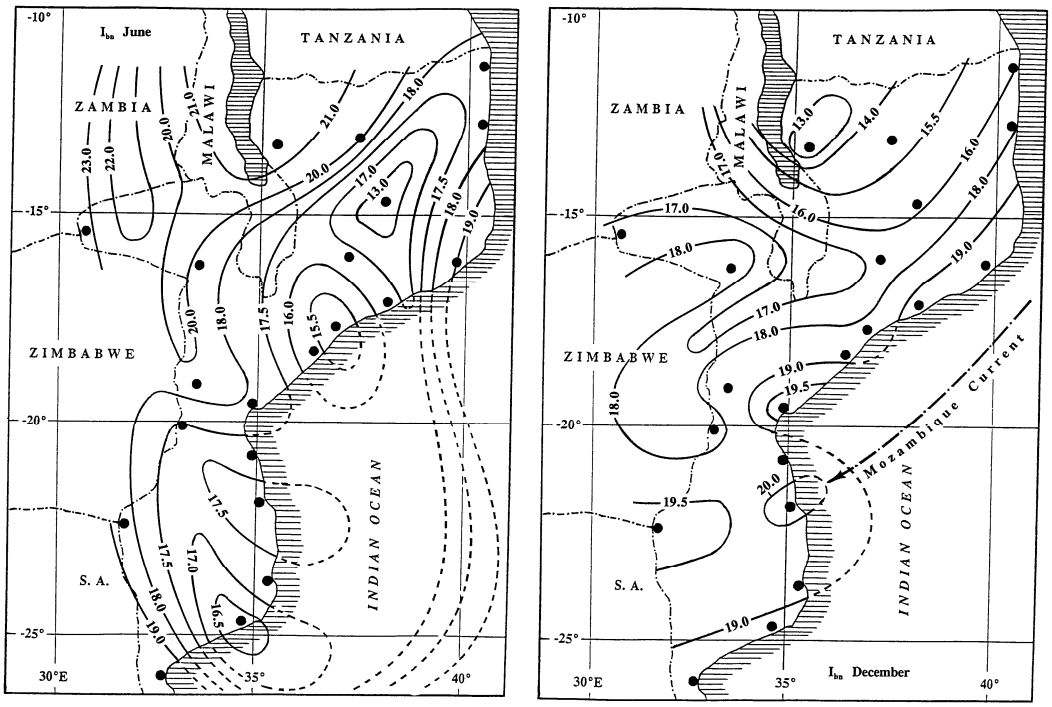

(a) (b)

Fig. 6 Maps showing monthly mean daily direct beam normal solar radiation (in MJ·m^{-2}) for (a) June and (b) December for Mozambique. The dots are the synoptic stations named in Fig. 3.

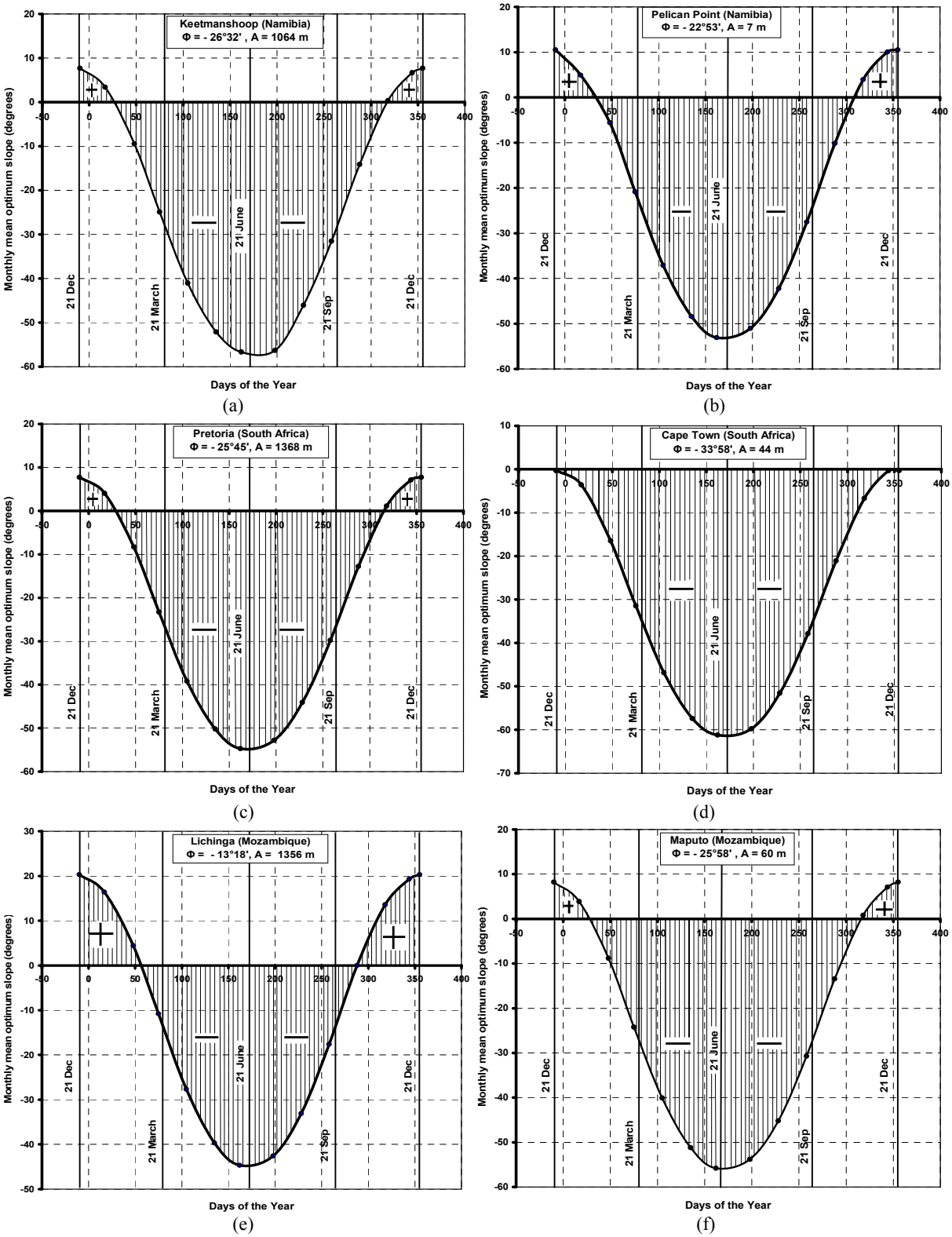

Fig. 7 Variation of the daily optimum slope with days of the year during clear cloudless weather for: (a) Keetmanshoop, (b) Pelican Point, (c) Pretoria, (d) Cape Town, (e) Lichinga, and (f) Maputo. The solid curves in this figure represent the variation of the daily optimum slopes with days of the year, the points/dots on the curve represent mean monthly optimum slopes, and the shaded areas represent the manifold of optimum slopes for different clear cloudless hours. (Monthly mean meteorological parameters were used in the simulations).

face to the South and the sign "-" means that the collector should face to the North. It is observed that the daily optimum slope is mainly determined by latitude, day of the year and sunshine hours. The optimum slope is at a maximum for completely cloudless days; with decreasing sunshine hours, daily optimum slope decreases and gets equal to zero if the sky dome is completely covered by clouds.

Analysis of results presented in Fig. 7 shows that for SADC countries optimum slope for a collector can either be positive or negative. At Cape Town (South Africa) location the optimum slope is zero for 21 December and negative for the rest of the dates, exceeding -60° for 21 June. The further one moves from Cape Town to the north, positive slopes are increasing and negative ones are decreasing. For example, at Lichinga (Mozambique) optimum slope for 21 December is equal to +20° and for 21 June it is equal to -45°. Simulated results which are not presented in this paper show that for the Equator, for example at Kisumu (Kenya) synoptic station, positive and negative optimum slopes are equally distributed, that is, during a half year (from 21 September to 21 March) optimum slopes are positive and during another half year (from 21 March to 21 September) they are negative. For 21 December the optimum slope is equal to +32° and for 21 June it is -32°, while for 21 March and 21 September the optimum slope is equal to zero. The results show that moving from the Equator further to the north, positive optimum slopes would continue to increase while the negative ones would be decreasing. Thus for latitudes $\phi \geq +33^{\circ}58^{'}$ optimum slopes are only positive. This is analogous to those for $\phi \leq -33^{\circ}58^{'}$ (i.e. from the latitude of Cape Town) where optimum slopes are only negative. Comparative analysis of the simulation results reveals that for SADC countries the range of variation of the optimum slope is from +30° (at the northern part of Tanzania on 21 December) to -62° (at Cape Town on 21 June). This information is important because if, for example, the slope of PV-arrays is corrected once in a month, the efficiency of this device would be boosted by at least 10-15%.

4. Conclusion

Experimental measurements of solar radiation conducted during more than 15 years at the University of Botswana main campus allowed to develop new algorithm and software to compute hourly, daily and mean monthly solar energy at any location of SADC countries using data of meteorological conditions. From the results obtained in this study the following conclusions are drawn.

(1) Botswana, Namibia, South Africa and Mozambique are extremely rich in solar energy.

(2) Continental areas are very much suitable for utilisation of solar energy using devices with concentrators (middle-temperature and high-temperature Rankine cycles), because in these locations usually H_{bn} component is much higher than in the coastal areas.

(3) Coastal areas are more suitable for utilisation of solar energy employing flat-plate collectors and PV-arrays.

(4) A very interesting correlation between prevailing trade winds and solar radiation patterns observed for Mozambique needs further investigation especially to compare with other countries with some coastlines.

(5) The mean monthly optimum slopes can be used to boost the efficiency of a PV-arrays by 10-15% if its slope would be corrected once in a month.

References

[1] K.K. Gopinathan, The distribution of global and sky radiation throughout Lesotho, Solar & Wind Technol. 5 (1) (1988) 103-106.

[2] J.K. Page, Estimation of monthly mean values daily total short-wave radiation on vertical and inclined surfaces from sunshine records for latitudes 40 North to 40 South, in: Proc. UN Conf. on New Sources of Energy, Rome, Italy, Paper No. S/98, 1961.

[3] K.K. Gopinathan, J. Mwanje, Estimation of solar radiation over Lesotho, INTERSOL 85 (1985) 23-29.

[4] K.K. Gopinathan, A general formula for computing the

coefficients of the correlation connecting global solar radiation to sunshine duration, Solar Energy 41 (6) (1988) 499-502.

[5] G. Lewis, Irradiance estimates for Zambia, Solar Energy 26 (1) (1981) 81-85.

[6] T. Hove, J. Göttsche, Mapping global, diffuse and beam solar radiation over Zimbabbwe, Renewable Energy 18 (4) (1999) 535-556.

[7] A. Madhlopa, Solar radiation climate in Malawi, Solar Energy 80 (8) (2006) 1055-1057.

[8] K.K. Gopinathan, N.B. Maliehe, M.I. Mpholo, A study on the intercepted insolation as a function of slope and azimuth of the surface, Energy 32 (3) (2007) 213-220.

[9] L. Diabaté, Ph. Blanc, L. Wald, Solar radiation climate in Africa, Solar Energy 76 (6) (2004) 733-744.

[10] N. Nijegorodov, K.R.S. Devan, P.K.J. Jain, S. Carlsson, Atmospheric transmittance models and an analytical method to predict the optimum slope of an absorber plate, variously oriented at any latitude, Renewable Energy 4 (5) (1994) 529-543.

[11] N. Nijegorodov, P.V.C. Luhanga, Air mass: Analytical and empirical treatment, an improved formula for air mass, Renewable Energy 7 (1) (1996) 57-65.

[12] N. Nijegorodov, P.V.C. Luhanga, A new model to predict direct normal instantaneous solar radiation, based on laws of spectroscopy, kinetic theory and thermodynamics, Renewable Energy 13 (4) (1998) 523-530.

[13] N. Nijegorodov, J.A. Adedoyin, K.R.S. Devan, A new analytical-empirical model for the instantaneous diffuse radiation and experimental investigation of its validity, Renewable Energy 11 (3) (1997) 341-350.

[14] N. Nijegorodov, P.K.J. Jain, Optimum slope of north-south aligned absorber plate from the North to the South Poles, Renewable Energy 11 (1) (1997) 107-118.

[15] J.A. Duffie, W. Beckman, Solar Engineering of Thermal Processes, 2nd ed., John Wiley and Sons, New York, USA, 1991.

[16] F. Kasten, A new table and approximate formula for relative optical air mass, Arch Meteorol Geophys Bioklimatol Ser B14 (1966) 206-223.

[17] T.K. van Heuklon, Estimating the atmospheric ozone for solar radiation models, Solar Energy 22 (1) (1979) 63-68.

[18] N.I. Nijegorodov, K.R.S. Devan, H. Simao, R. Mabbs, Comprehensive study of solar conditions in Mozambique: The effects of trade winds on solar components, Renewable Energy 28 (12) (2003) 1965-1983.